A Novel Rapid Iterative Algorithm and Its Application on Clinical Diagnosis of Coronary Artery Disease

Technical Memorandum by

Nazarbayev University, Kazakhstan

AND

Dalian University of Technology, China

August, 2018

Contents

I. METHODOLOGY

A. The Murray's Law

The Hagen–Poiseuille equation (Hagen, 1839; Sutera & Skalak, 1993), experimentally derived by Jean Léonard Marie Poiseuille in 1838 and Gotthilf Heinrich Ludwig Hagen in 1839 independently, is a physical law that gives the pressure drop in an incompressible and Newtonian fluid in laminar flow flowing through a long cylindrical pipe of constant cross section.

In standard fluid-dynamics notation, the equation reads:

$$\Delta p = \frac{8\mu LQ}{\pi r^4} = \frac{128\mu LQ}{\pi d^4} = \frac{32\mu LV}{\pi d^2} \tag{1}$$

where Δp is the pressure difference between the two ends, μ is the dynamic viscosity, L is the length of pipe, Q is the volumetric flow rate, r is the pipe radius, d is the pipe diameter, V is the averaged velocity of cross section.

Eq. (1) is extended to the field of human coronary artery vascular system (Figure 1), known as the Murray's law (Murray, 1926), which indicates the mathematical relationship between vessel size and volumetric flow rate (Taylor, Fonte, & Min, 2013):

$$Q = \frac{\pi}{32\mu}\tau_{\omega} d^3 \tag{2}$$

where τ_{ω} is the wall shear stress of a vascular, maintained at a constant, homeostatic level.

Thus, Eq. (2) implies:

$$Q \propto d^3 \tag{3}$$

Therefore, a general relationship of conservative volumetric flow rate distribution in a vascular system with *n* outlet branches (Figure 2) is expressed as:

$$Q = \sum_{i=1}^{n} Q_i = \sum_{i=1}^{n} \alpha_i Q = \sum_{i=1}^{n} \frac{d_i^3}{d_1^3 + d_2^3 + \cdots + d_n^3} Q \tag{4}$$

where *n* is the total number of branches, *i* is the outlet index, Q_i is the volumetric flow rate of the No. *i* branch, d_i is the diameter of the No. *i* branch, $\alpha_i = d_i^3 \big/ \left(d_1^3 + d_2^3 + \cdots + d_n^3\right)$ is the proportionality coefficient of the No. *i* branch.

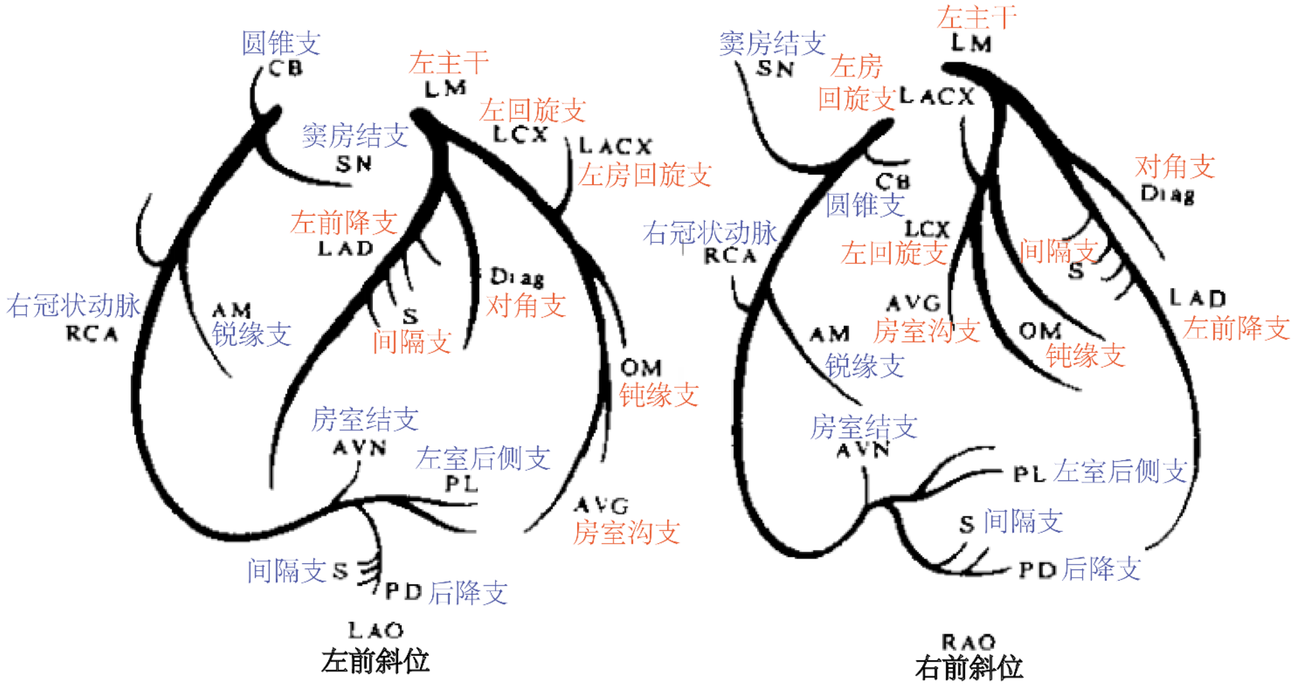

Figure 1 Sketch of human coronary artery

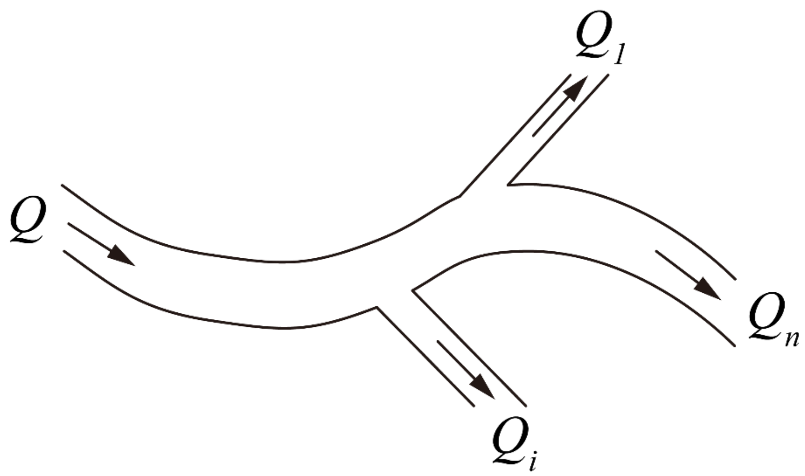

Figure 2 Sketch of volumetric flow rate distribution

B. The Rapid Iterative Algorithm

Figure 3 shows the workflow of the rapid iterative algorithm. Super- and subscripts of variables in Figure 3 are defined as follows: *i* is the outlet index, *j* is the iteration index.

(1) Obtain the computational domain, static pressure p and volumetric flow rate Q of the inlet boundary by proceeding coronary computed tomography angiography (CTA).

(2) Evaluate the initial volumetric flow rate distribution of outlets $Q_i = \alpha_i Q$ using the Murray's law.

(3) When j = 1, load p and Q_i onto the inlet and outlet boundary conditions respectively. Where after, the static pressure distribution of outlets $p_i^{[1]}$ will be gathered while a steady-state CFD

solving is processed. Replace the inlet and outlet boundary conditions with Q and $p_i^{[1]}$ respectively, and resolve the steady-state CFD issue. The static pressure of inlet $p^{[1]}$ and volumetric flow rate distribution of outlets $Q_i^{[1]}$ will be gathered.

(4) Check the stop condition $\left|\left(p^{[j]}-p\right)/p\right| \leq \delta$.

(5) Redo the steps (3) and (4), until the stop condition is fully met.

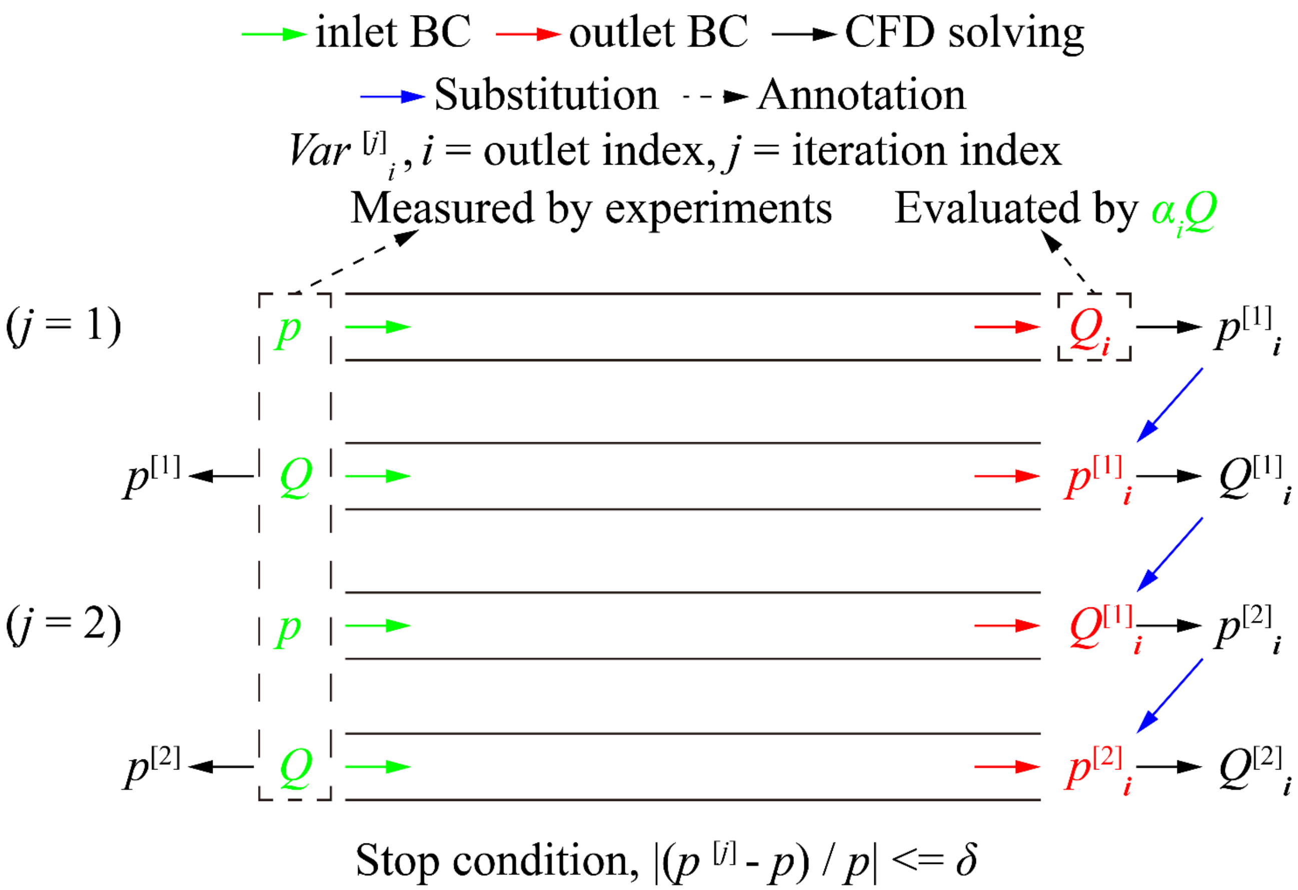

Figure 3 Workflow of the rapid iterative algorithm

II. NUMERICAL CASE

Three numerical cases in Figure 4 (Zhang, Zhong, & Luo, et al., 2016) are set-up to validate the rapid iterative algorithm using parameters listed in Table 1. The initial proportionality coefficient distribution of outlets α_i is highlighted in Table 2.

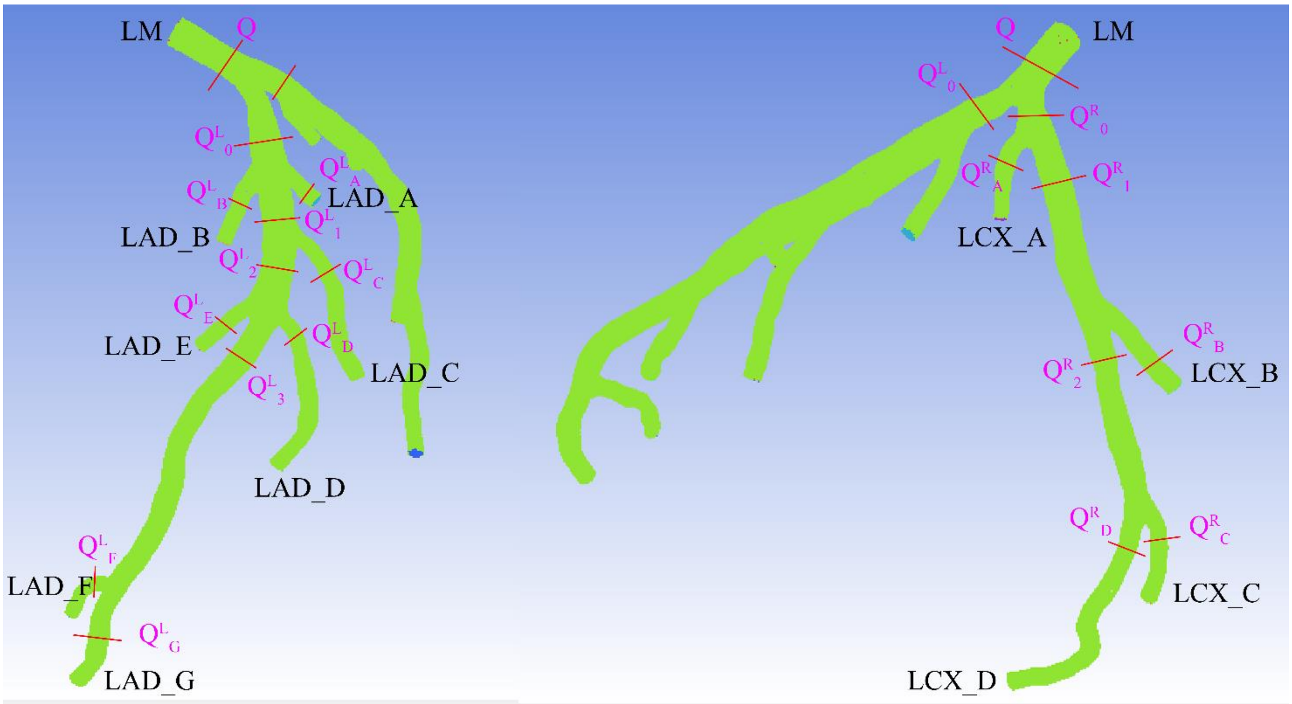

Figure 4 Computational domain of left coronary artery with 1 inlet and 11 outlets, the digital extraction of computed tomography angiography (CTA)

Table 1 Parameters of the numerical cases

<table>
<tr><th>Case</th><th colspan="4">Solver</th></tr>
<tr><td>1</td><td colspan="4">Results from Junmei's Tecplot file</td></tr>
<tr><td>2</td><td colspan="4">Results of present model by using CFX</td></tr>
<tr><td>3</td><td colspan="4">Results of present model by using Fluent</td></tr>
<tr><th>Item</th><th colspan="4">Value</th></tr>
<tr><td>Geometry</td><td colspan="4">Left coronary artery</td></tr>
<tr><td>Cell</td><td colspan="4">649247</td></tr>
<tr><td rowspan="2">Inlet</td><td rowspan="2">LM</td><td>Flow Rate (m^3 s^{-1})</td><td>Static Pressure (Pa)</td><td>Total Pressure (Pa)</td></tr>
<tr><td>6.19E-06</td><td>9981.40368</td><td>10240.77688</td></tr>
<tr><td>Outlet</td><td colspan="4">LAD_(A~G) + LCX_(A~D)</td></tr>
</table>

Table 2 Initial proportionality coefficient distribution of outlets for case2 and case3

Initial Volume Flow Rate						Perimeter	Diameter	Initial α_i						$\Sigma\ \alpha_i$
Lv. Root	Lv. 0	Lv. 1	Lv. 2	Lv. 3	Lv. 4	m	m	Lv. Root	Lv. 0	Lv. 1	Lv. 2	Lv. 3	Lv. 4	
Q						0.009871	0.003142	1						1
	Q_0^L					0.008061	0.002566		0.401027					
		Q_A^L				0.005533	0.001761			0.033047				0.033047
		Q_B^L				0.006219	0.001980			0.046944				0.046944
		Q_1^L				0.011805	0.003758			0.321036				
			Q_C^L			0.005109	0.001626				0.027074			0.027074
			Q_2^L			0.011314	0.003601				0.293963			
				Q_D^L		0.004924	0.001567					0.035465		0.035465
				Q_E^L		0.005305	0.001689					0.044352		0.044352
				Q_3^L		0.008966	0.002854					0.214146		
					Q_F^L	0.005522	0.001758						0.078319	0.078319
					Q_G^L	0.006634	0.002112						0.135826	0.135826
	Q_0^R					0.009214	0.002933		0.598973					
		Q_A^R				0.005203	0.001656			0.107381				0.107381
		Q_1^R				0.008640	0.002750			0.491591				
			Q_B^R			0.005451	0.001735				0.140581			0.140581
			Q_2^R			0.007395	0.002354				0.351011			
				Q_C^R		0.005080	0.001617					0.135897		0.135897
				Q_D^R		0.005921	0.001885					0.215114		0.215114

III. RESULTS AND DISCUSSION

Figures 5~7 are the static pressure contour of the 3 numerical cases, and the detailed values are listed in Table 3 for parallel comparison.

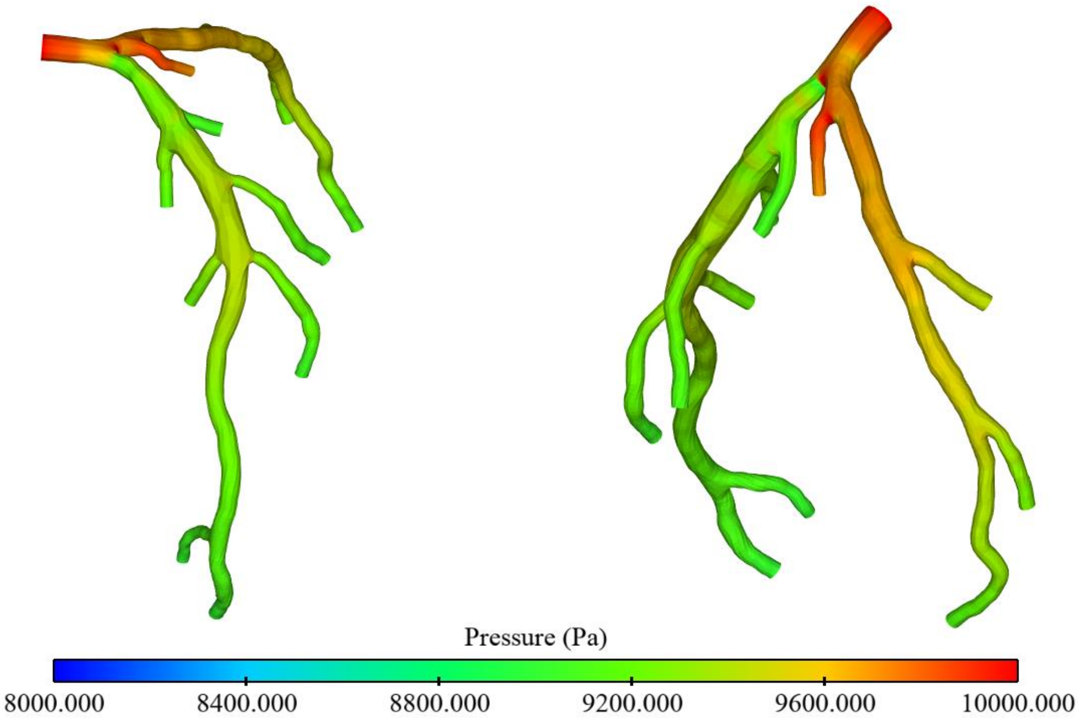

Figure 5 Static pressure of Case 1

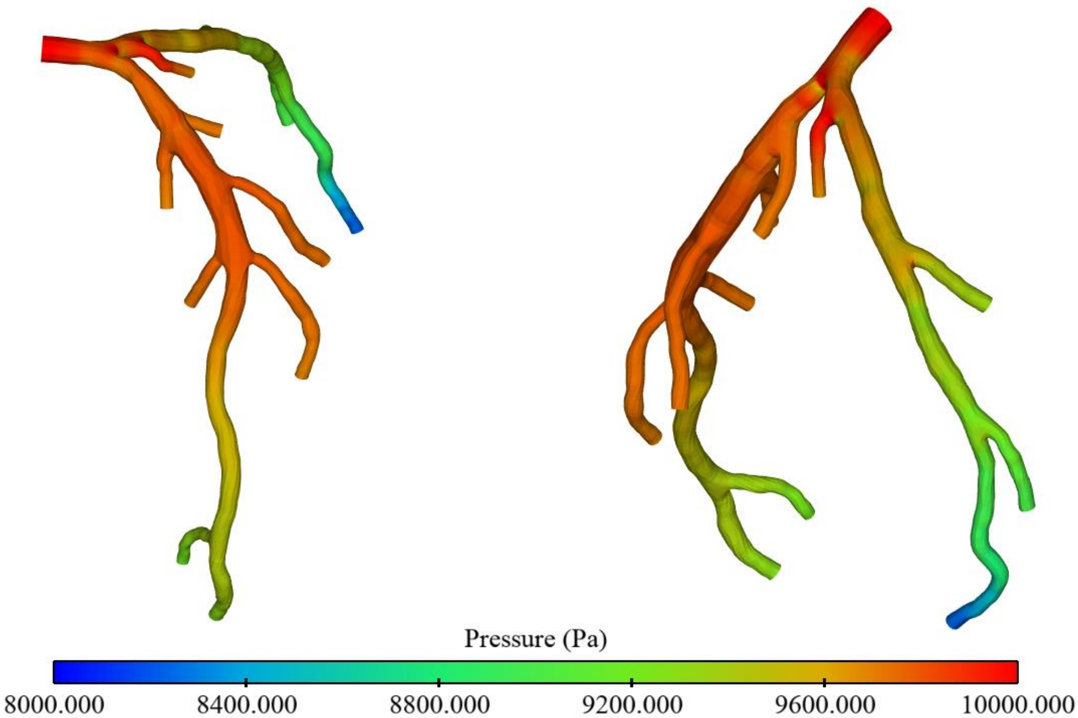

Figure 6 Static pressure of Case 2

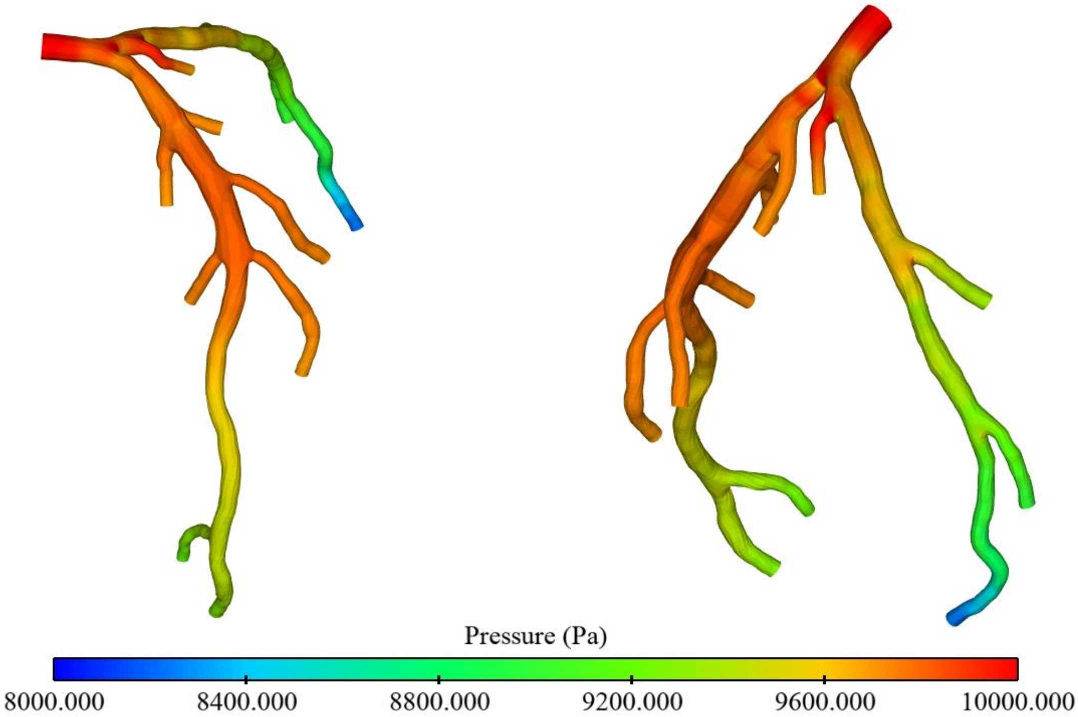

Figure 7 Static pressure of Case 3

Table 3 Comparison table of the numerical cases

Item		Case 1	Case 2		Case 3	
		Static Pressure (Pa)	Static Pressure (Pa)	Flow Rate (m^3 s^{-1})	Static Pressure (Pa)	Flow Rate (m^3 s^{-1})
Inlet	LM	1.010E+04	10060	6.188E-06	10116	6.186E-06
Outlet	LAD_A	9.064E+03	9703	2.187E-07	9703	2.029E-07
	LAD_B	9.134E+03	9678	3.088E-07	9678	2.956E-07
	LAD_C	9.089E+03	9716	1.882E-07	9716	2.067E-07
	LAD_D	9.040E+03	9678	2.368E-07	9678	2.649E-07
	LAD_E	9.208E+03	9704	2.982E-07	9704	3.334E-07
	LAD_F	8.986E+03	9158	4.861E-07	9158	4.756E-07
	LAD_G	9.003E+03	9270	8.609E-07	9270	8.847E-07
	LCX_A	9.669E+03	9647	5.780E-07	9647	5.465E-07
	LCX_B	9.419E+03	9335	8.526E-07	9335	8.636E-07
	LCX_C	9.238E+03	8999	8.303E-07	8999	8.469E-07
	LCX_D	9.120E+03	8245	1.326E-06	8245	1.265E-06

IV. REFERENCES

Hagen, G. (1839). Ueber die Bewegung des Wassers in engen cylindrischen Röhren. *Annalen Der Physik*, *122*(3), 423-442.

Murray, C. D. (1926). The physiological principle of minimum work: I. The vascular system and the cost of blood volume. *Proceedings of the National Academy of Sciences*, *12*(3), 207-214.

Sutera, S. P., & Skalak, R. (1993). The history of Poiseuille's law. *Annual Review of Fluid Mechanics*, *25*(1), 1-20.

Taylor, C. A., Fonte, T. A., & Min, J. K. (2013). Computational fluid dynamics applied to cardiac computed tomography for noninvasive quantification of fractional flow reserve: Scientific basis. *Journal of the American College of Cardiology*, *61*(22), 2233-2241.

Zhang, J., Zhong, L., & Luo, T. (2016). Simplified models of non-invasive fractional flow reserve based on CT images. *Plos One*, *11*(5), e153070.